282, 33 (1970).
(17) J. J. Rahal, M. S. Simberkoff, and P. J. Hyams, *J. Infect. Dis., Suppl.*, 128, 762 (1973).
(18) R. M. E. Richards and R. J. McBride, *J. Pharm. Sci.*, 61, 1075 (1972).
(19) *Ibid.*, 62, 585 (1973).
(20) *Ibid.*, 62, 2035 (1973).
(21) *Ibid.*, 63, 54 (1974).
(22) R. M. E. Richards and R. H. Cavill, *J. Pharm. Sci.*, 65, 76 (1976).
(23) R. M. E. Richards and R. H. Cavill, *J. Pharm. Pharmacol.*, 28, 935 (1976).
(24) M. R. W. Brown and R. M. E. Richards, *ibid.*, 16, 41T (1964).
(25) R. M. E. Richards and R. J. McBride, *ibid.*, 23, 141S (1971).
(26) R. M. E. Richards and L. M. Mizrahi, *J. Pharm. Sci.*, 67, 380 (1978).
(27) M. R. W. Brown and R. M. E. Richards, *J. Pharm. Pharmacol.*, 16, 51T (1964).
(28) R. M. E. Richards, *ibid.*, 23, 136S (1971).
(29) *Ibid.*, 30, 14P (1978).

Urinary Iodine Excretion Rates following Intrathecal Injections of Iodinated Organic Carbonates

A. E. STAUBUS *x, B. N. NEWTON ‡, L. C. KLEIN ‡, A. B. WEINRIB *, and A. L. KUNZ ‡

Received May 17, 1978, from the **College of Pharmacy, Ohio State University, Columbus, OH 43210,* and the ‡*Research and Development Department, Lafayette Pharmacal, Division of Alcon Laboratories, Inc., Lafayette, IN 47902.* Accepted for publication June 4, 1979.

Abstract □ Oily iodinated organic carbonates were investigated for use as myelographic media. The urinary excretion of total iodine was used to monitor the apparent elimination rate of these compounds from the subarachnoid space. Within the chain length series of C_2–C_6, the decrease of elimination rates and disposition rate constants with increasing chain length was demonstrated. This observation is consistent with a dissolution rate-limited elimination model. Such a model was derived and successfully NONLIN computer fitted to the observed elimination data. The model-derived parameter of clearance from the cerebrospinal fluid through the lipid "blood–brain barrier" correlated well with the compound's water solubilities and projected octanol–water partition coefficients. Additional compounds need to be tested to evaluate the postulated model system.

Keyphrases □ Myelographic agents—oily iodinated organic carbonates, biological elimination □ Pharmacokinetics—myelographic agents, oily iodinated organic carbonates, biological elimination □ Contrast media—oily iodinated organic carbonates, biological elimination

Positive-contrast myelography is the X-ray visualization of the subarachnoid space using a radiopaque substance. It is used to evaluate trauma to the spinal column and to delineate tumors and other canal obstructions. The only approved myelographic agent in the United States is iophendylate [ethyl 10-(*p*-iodophenyl)undecylate[1]] (I).

Iophendylate has been used in the United States in several million examinations since the early 1940's. It is considered to be very safe; however, it is removed at the conclusion of the examination because its biological elimination has been reported to be 1 ml/year (1). Water-soluble contrast agents have been used in Europe for over 30 years, but they have not been approved for use in the United States due to their higher incidence of adverse reactions.

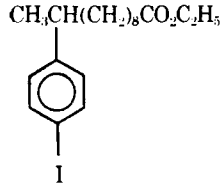

I

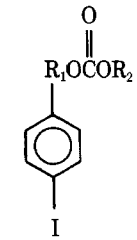

II

$R_1 = -(CH_2)-_n$, n = 0–4
$R_2 = -C_nH_{2n+1}$, n = 1–10

Drawbacks with the current agents necessitated a search for a readily absorbable, nontoxic, oily myelographic medium. Oily iodinated organic carbonates of the general Structure II (2) were investigated. To understand quantitatively the biological elimination of these compounds, four representative carbonates were selected for study.

EXPERIMENTAL

The urinary excretion of total iodine was used to monitor the apparent elimination rate of the four carbonates from the subarachnoid space. In preliminary studies, the rate-limiting step for the overall elimination of compounds from the body appeared to be absorption from the subarachnoid space.

In an additional study, a series of rats was sacrificed at 24, 48, and 72 hr and on Day 5 following suboccipital injection. Other than expected high brain tissue levels, the only detectable iodine concentrations were in trace amounts (~0.3 μmole/g) found in skin samples at 24, 48, and 72 hr. Heart, kidney, liver, leg muscle, lung, and intestine samples on any of the 4 days and Day 5 skin samples all showed no detectable iodine. Consequently, the urinary excretion of the iodinated metabolites should reflect the relative absorption rates. For statistical purposes, each of the four compounds was tested in six rats. This method quantitatively confirmed the radiographic disappearance observed in these animals.

Thirty-six adult Sprague–Dawley female rats, 197–225 g, were divided into six equal groups. Each group was dosed with a different test compound. The purity of each test compound (Table I) was determined by GLC and NMR and agreed with analytically pure samples (~99% pure).

[1] Pantopaque.

0022-3549/79/1100-1438$01.00/0

Table I—Physical Properties of *p*-Iodobenzyl Carbonates

Compound	R_1	R_2	Viscosity[a] at 25°, cps	Density	n_D^{25}	Water Solubility, mole/liter	Molecular Formula	Analysis, % Calc.	Found
II*a*	$-CH_2-$	$-C_2H_5$	11.76	1.6108	1.5587	6×10^{-5}	$C_{10}H_{11}IO_3$	C 39.22	39.24
								H 3.62	3.77
								I 41.48	41.49
II*b*	$-CH_2-$	$-C_4H_9$	14.37	1.4959	1.5431	1.3×10^{-5}	$C_{12}H_{15}IO_3$	C 43.11	42.87
								H 4.53	4.40
								I —[b]	—[b]
II*c*	$-CH_2-$	$-C_5H_{11}$	16.68	1.4584	1.5439	2.8×10^{-6}	$C_{13}H_{17}IO_3$	C 44.82	44.50
								H 4.92	4.84
								I 36.46	37.51
II*d*	$-CH_2-$	$-C_6H_{13}$	18.58	1.4100	1.5368	1.9×10^{-6}	$C_{14}H_{19}IO_3$	C 46.40	46.25
								H 5.29	5.36
								I 35.05	34.77

[a] Ostwald viscosity technique. [b] Not available.

Table II—Reproducibility of Urinary Iodine Concentrations

Standard, μmole/ml	Mean Concentration, μmoles/ml	*CV*, %
0.15	0.149	12.0
0.25	0.218	10.2
0.50	0.553	5.5
1.00	1.019	3.0

Table III—Daily Means and Standard Deviations for Cumulative Urinary Excretion of II*a* (Micromoles per Kilogram)

Day	Mean	*SD*
1	354.7	105.4
2	935.1	114.9
3	1237.4	119.8
4	1306.1	143.2
5	1345.9	155.6
6	1358.9	161.7
7	1367.5	166.7
8→∞	1372.7	170.1

The animals were removed from feed 18 hr before dosing. After anesthetization with ether, the back of the neck was clipped closely. The animal was then placed on a grooved board that allowed the head to be declined at 45°. With a 27-gauge needle, a puncture was made at the base of the atlas and 2.5 mmoles/kg of the test material was injected uniformly over 15 sec. Suboccipital injection was confirmed radiographically. The animals were then placed in individual metabolism cages, and the urine was collected at 24-hr intervals until the urine concentrations dropped below the assay reliability.

Individual rat urine volumes were measured in 50-ml graduated cylinders, and representative 1.5-ml aliquots were removed and transferred to disposable plastic analyzer cups[2]. The daily urinary iodine concentration of each rat was determined using k-shell fluorescent activation analysis (3). The reproducibility of eight replicates of four representative concentrations is shown in Table II.

RESULTS AND DISCUSSION

Daily Urinary Excretion Rate Variability—Figures 1A and 1B illustrate the urinary excretion rate variability for individual rats. The correlation coefficient (r) of the terminal log-linear disposition phases ranged from $r > 0.99$ (Fig. 1A) to $r > 0.88$ (Fig. 1B). In general, correlation coefficients were >0.96.

Mean Urinary Excretion Rate Data—As can be seen from the mean urinary excretion rate plots (Figs. 2–5), peak iodine excretion rates occurred within 1–2 days following intrathecal administration. With increasing chain length of the R_2 group (II), the terminal log-linear half-life ($t_{1/2}$) progressively increased. The terminal $t_{1/2}$ values ranged from 0.78 day for II*a* to 11.3 days for II*d*.

Cumulative Urinary Excretion Data—The same relative correlation with chain length can be seen in both the mean cumulative urinary excretion plot (Fig. 6) and the plot of the percent remaining to be eliminated (Fig. 7). Intersubject variability can be evaluated from the means and standard deviations provided in Tables III–VI for the cumulative urinary excretion of these compounds. Compound II*c* had the least intersubject variability.

For all four compounds, the percent of the dose excreted into the urine was essentially identical (54.9 ± 0.9%). Since no radiopaque residues were observed at the end of each study, the remaining dose was presumed to be eliminated *via* the biliary fecal route. Spot checking of fecal samples for iodine content confirmed the biliary excretion component of elimination.

Terminal Disposition Rate Constants—The mean, standard deviation, and corresponding $t_{1/2}$ values for the terminal disposition rate constants are shown in Table VII. Again, the influence of increasing the chain length of the alkyl portion of the molecule was reflected in dramatic changes in the magnitude of the terminal disposition rate constants and in the harmonic means of their corresponding $t_{1/2}$ values.

Table IV—Daily Means and Standard Deviations for Cumulative Urinary Excretion of II*b* (Micromoles per Kilogram)

Day	Mean	*SD*	Day	Mean	*SD*
1	283.5	32.6	12	1242.4	148.8
2	538.0	43.0	13	1266.4	153.1
3	712.3	78.0	14	1285.2	156.5
4	815.0	97.0	15	1303.3	158.5
5	905.1	113.9	16	1316.1	160.9
6	991.7	119.1	17	1328.6	162.5
7	1053.4	127.3	18	1337.9	165.9
8	1104.7	129.7	19	1347.1	169.7
9	1149.9	134.6	20	1354.3	171.5
10	1187.7	140.3	21	1360.5	172.9
11	1215.6	145.5	22→∞	1398.0	187.2

Table V—Daily Means and Standard Deviations[a] for Cumulative Urinary Excretion of II*c* (Micromoles per Kilogram)

Day	Mean	*SD*	Day	Mean	*SD*
1	280.9	69.3	19	1284.3	93.5
2	505.1	108.5	20	1294.0	93.9
3	656.8	113.7	21	1303.9	93.3
4	755.9	95.4	22	1311.8	93.2
5	842.5	95.1	23	1318.8	93.5
6	930.6	85.9	24	1324.9	93.6
7	989.3	94.5	25	1330.2	93.5
8	1037.2	103.1	26	1335.4	93.2
9	1079.1	100.8	27	1340.1	93.0
10	1121.2	97.1	28	1343.7	92.4
11	1153.2	96.9	29	1346.3	91.6
12	1173.4	97.9	30	1349.6	90.8
13	1196.2	97.5	31	1352.3	90.2
14	1215.6	95.9	32	1354.8	90.2
15	1233.3	95.0	33	1357.4	90.1
16	1247.1	94.1	34	1360.2	89.1
17	1262.0	93.4	35	1362.0	88.8
18	1274.6	93.3	36→∞	1377.0	84.1

[a] The reported values for II*c* pertain to the mean and standard deviation of only five of the six administered rats. One rat had to be rejected based on radiographic evidence of subcutaneous injection instead of intrathecal injection and its grossly dissimilar elimination behavior.

[2] Sherwood Medical Industries, St. Louis, Mo.

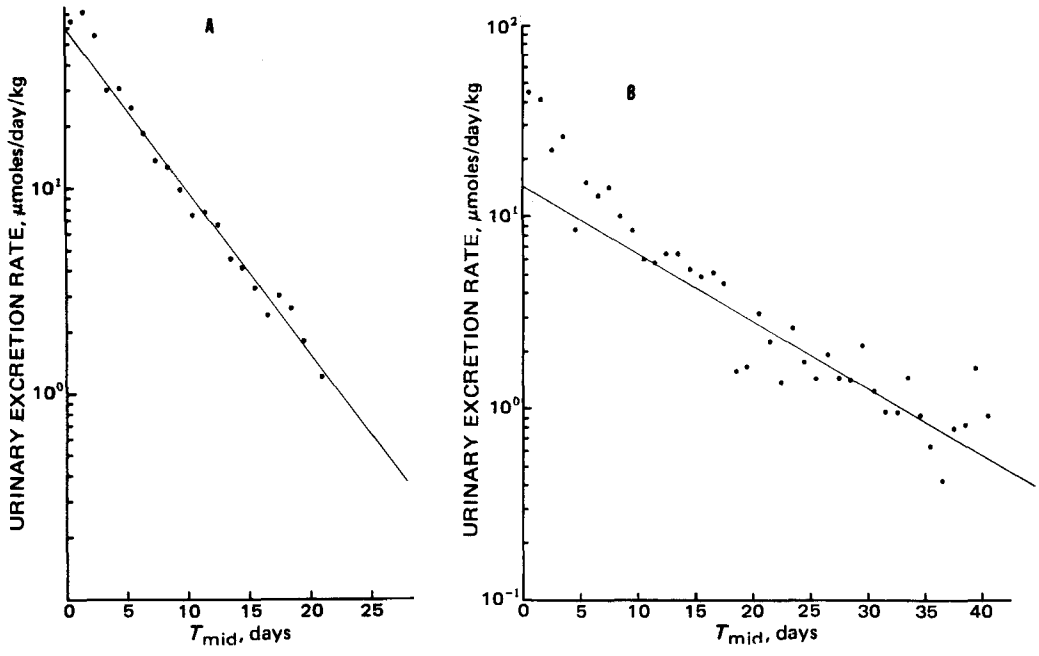

Figure 1—*A. Example of the best individual rat's urinary excretion rate plot. Compound IIb was administered. Straight line and corresponding half-life value were derived from log-linear regression of terminal data points. B. Example of the worst individual rat's urinary excretion rate plot. Compound IId was administered. Straight line and corresponding half-life value were derived from log-linear regression of terminal data points.*

Pharmacokinetic Model Fitting—Based on the extremely low water solubilities of the compounds and the apparent correlation of the amounts remaining to be eliminated with X-ray evidence of the oil droplets adhering to the spinal cord, an attempt was made to computer fit the excretion data with a dissolution rate-limited elimination mode. The model chosen incorporated the following assumptions:

1. The rate-limiting step for the overall elimination from the body was the oil dissolution into the aqueous environment of the cerebrospinal fluid (CSF).
2. Following oil dissolution into the cerebrospinal fluid, diffusion and cerebrospinal fluid circulation carried the dissolved compound to an absorption surface ("blood–brain barrier"), where the dissolved drug was cleared rapidly by a passive first-order mechanism into the venous circulation system.
3. The subsequent metabolism and excretion of the compounds were rapid and nonrate limited, permitting the daily elimination rate to approximate the daily flux of the compound from the cerebrospinal fluid.

Passage through the blood–brain barrier can be represented pharmacokinetically by:

$$\frac{dA_e}{dt} = (Cl_{CSF})(C) \qquad \text{(Eq. 1)}$$

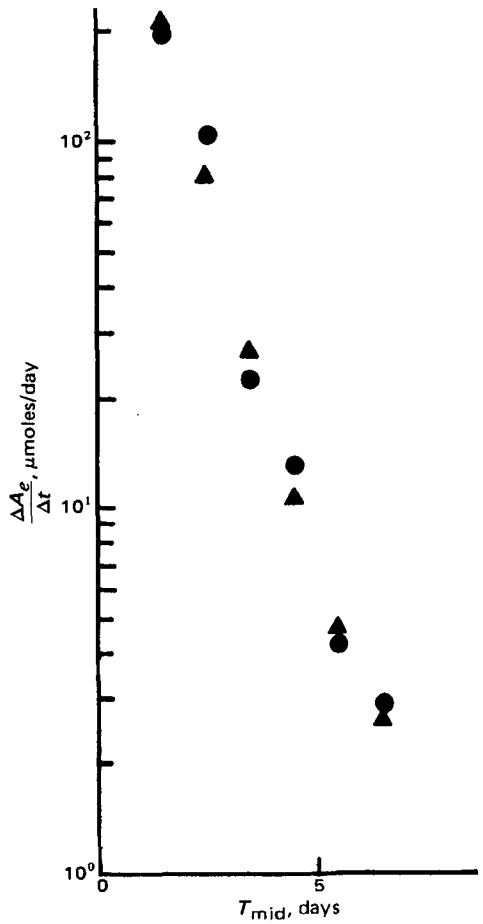

Figure 2—*Predicted (▲) and observed (●) elimination rates* versus *midpoint times for IIa.*

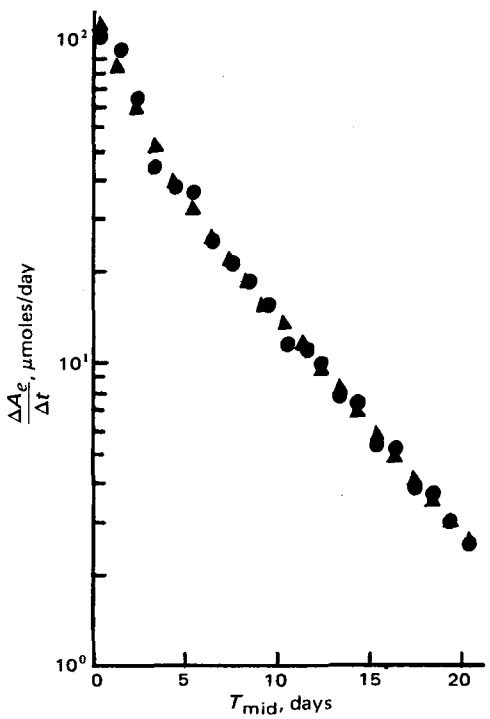

Figure 3—*Predicted (▲) and observed (●) elimination rates* versus *midpoint times for IIb.*

Table VI—Daily Means and Standard Deviations for Cumulative Urinary Excretion of II*d* (Micromoles per Kilogram)

Day	Mean	*SD*	Day	Mean	*SD*
1	270.3	93.2	22	1148.5	251.7
2	436.8	95.0	23	1159.0	251.3
3	537.5	84.8	24	1169.7	251.1
4	629.1	163.6	25	1181.9	252.0
5	687.9	163.6	26	1190.3	251.3
6	755.0	191.0	27	1198.7	252.0
7	814.5	203.4	28	1207.1	251.9
8	863.9	217.3	29	1215.3	252.2
9	903.5	227.5	30	1223.0	252.1
10	937.6	227.7	31	1230.5	251.6
11	962.9	230.0	32	1237.8	251.2
12	987.1	232.8	33	1243.0	251.4
13	1008.5	235.5	34	1248.8	250.6
14	1029.9	238.7	35	1254.3	249.7
15	1049.8	241.5	36	1259.2	248.8
16	1068.7	245.5	37	1263.3	249.2
17	1085.1	245.7	38	1267.7	249.2
18	1099.9	247.0	39	1271.7	249.2
19	1110.8	247.2	40	1276.7	248.4
20	1122.5	247.6	41	1280.9	247.9
21	1137.5	250.7	42→∞	1343.2	236.5

where:

$\frac{dA_e}{dt}$ = average total daily elimination rate (calculated from fraction excreted) or average daily flux from the cerebrospinal fluid (grams per day)

Cl_{CSF} = cerebrospinal fluid clearance through the blood–brain barrier (liters per day)

C = concentration of the compound at the absorption surface of the blood–brain barrier (grams per cubic centimeter)

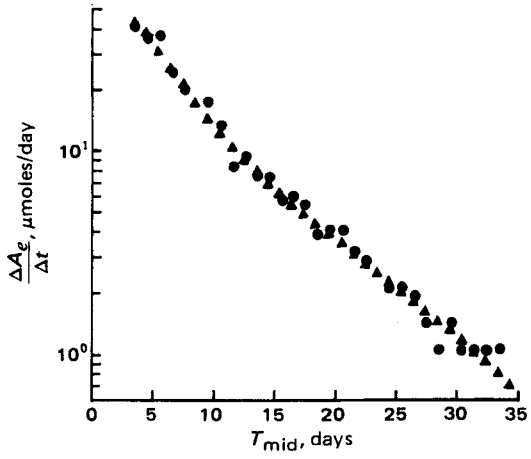

Figure 4—*Predicted (▲) and observed (●) elimination rates* versus *midpoint times for II*c.

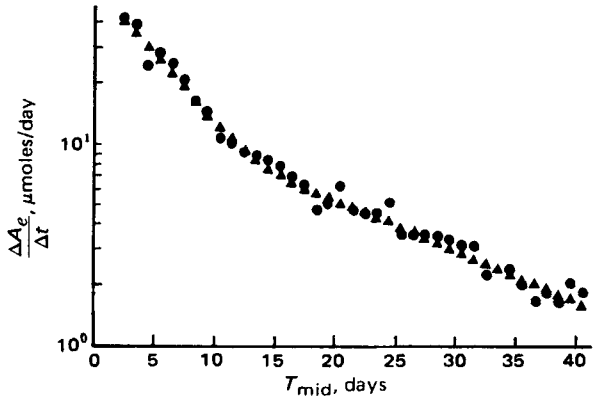

Figure 5—*Predicted (▲) and observed (●) elimination rates* versus *midpoint times for II*d.

Table VII—Mean, Standard Deviation, and Corresponding $t_{1/2}$ Values for the Terminal Disposition Rate Constants

Compound	Disposition Rate Constant, day^{-1} Mean	*SD*	$t^*_{1/2}$[a], days (Range of Individual $t_{1/2}$ Values)
II*a*	0.9273	0.1605	0.75 (0.63–0.95)
II*b*	0.1755	0.0385	3.95 (3.02–5.24)
II*c*	0.1147	0.0143	6.04 (5.47–7.58)
II*d*	0.0630	0.0144	10.99 (8.26–14.59)

[a] $t^*_{1/2}$ = (0.693/mean terminal disposition rate constant).

Selection of the dissolution rate-limited model allows use of the Noyes–Whitney equation (4):

$$\frac{dA_e}{dt} = \frac{AD}{h}(C_s - C) \qquad \text{(Eq. 2)}$$

where dA_e/dt and C are the same as already given, A is the average daily surface area of oil droplets (square centimeters), D is the diffusion coefficient of the compound through the cerebrospinal fluid (square centimeters per day), h is the average effective diffusion layer thickness (centimeters), and C_s is the water solubility of the compound (grams per cubic centimeter).

Since both Eqs. 1 and 2 share the term C, they can be rearranged into the following equation for the average daily elimination rate:

$$\frac{dA_e}{dt} = \left(\frac{C_s}{\frac{1}{Cl_{CSF}} + \frac{1}{(AD/h)}}\right) \qquad \text{(Eq. 3)}$$

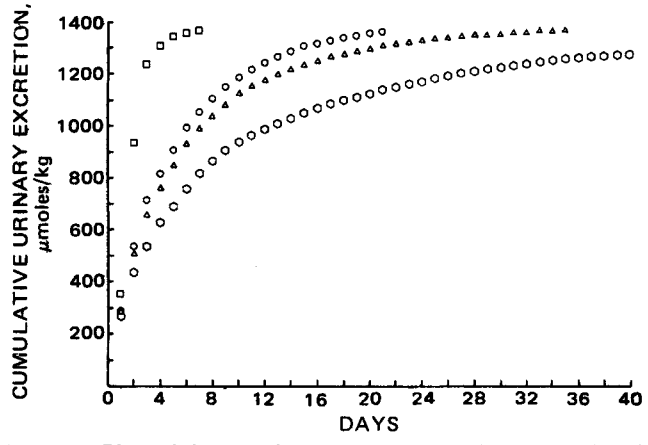

Figure 6—*Plots of the cumulative urinary excretion* versus *time for each of the four compounds.*

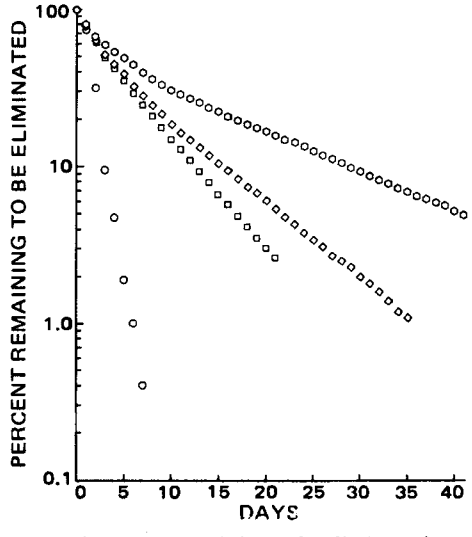

Figure 7—*Plots of percent remaining to be eliminated* versus *time for each of the four compounds.*

Table VIII—Estimates for the Dissolution Rate-Limited Model

Compound	$A \times 10^{-12}$, cm³/day³	$B \times 10^{-12}$, cm³/day³	α, days^{-1}	β, days^{-1}	$Cl \times 10^{-4}$, ml/day
II*a*	4.723	1.997×10^{-3}	1.629	3.497×10^{-2}	1.121
II*b*	3.954	2.142×10^{-1}	0.9686	1.819×10^{-1}	2.417
II*c*	250.0	3.136	0.5387	1.143×10^{-1}	3.562
II*d*	326.0	1.393	0.5357	6.619×10^{-2}	3.908

Table IX—Comparison of Weighted Sum of Squares Deviations

Compound	Dissolution Rate-Limited Model	Model-Independent Biexponential
II*a*	0.1236	0.1654
II*b*	0.1148	0.1280
II*c*	0.4566	0.4604
II*d*	0.4678	0.4978

Equation 3 accurately predicts the expected elimination rate for two possible extreme conditions: (*a*) if the amount of oil injected into the cerebrospinal fluid is extremely large, then with a large surface area, $[1/(AD/h)]$ will be overshadowed by $[1/(Cl_{CSF})]$, resulting in a pseudo-zero-order elimination rate of $(Cl_{CSF})(C_s)$; and (*b*) if the amount of oil remaining within the cerebrospinal fluid approaches zero, $[1/(AD/h)]$ will approach infinity and will overshadow $[1/(Cl_{CSF})]$, resulting in an elimination rate of nearly zero.

To utilize Eq. 3, it is necessary to approximate the average daily surface area. It can be calculated based on the average daily amount remaining to be eliminated $[(ARE_i + ARE_{i-1})/2]$, the oil density, the apparent average daily number of oil droplets (n), and the assumption of spherical oil drops. The resulting surface area equation is:

$$A = \left(\frac{9\pi n}{\text{density}^2}\right)^{1/3} (ARE_{i-1} + ARE_i)^{2/3} \qquad \text{(Eq. 4)}$$

By substitution of Eq. 4 into Eq. 3, Eq. 5 results:

$$\frac{dA_e}{dt} = \frac{C_s}{\dfrac{1}{Cl_{CSF}} + \dfrac{1}{\left[\left(\dfrac{D}{h}\right)^3 n\right]^{1/3} \left(\dfrac{9\pi}{\text{density}^2}\right)^{1/3} (ARE_{i-1} + ARE_i)^{2/3}}} \qquad \text{(Eq. 5)}$$

Knowing *in vitro* determinations of C_s and density (Table I) and *in vivo* determinations of dA_e/dt and ARE values, Eq. 5 can be NONLIN (5) fitted to solve for Cl_{CSF} and $(D/h)^3n$. Initial NONLIN fitting of Eq. 5 using 5-day segments of II*d* revealed that the Cl_{CSF} parameter remained essentially constant throughout the 41-day study while $[(D/h)^3n]$ decreased with increasing time. The decrease in $[(D/h)^3n]$ was found to fit empirically a simple biexponential equation. Consequently, the standard biexponential equation $[(D/h)^3n] = (A_e^{-\alpha t} + B_e^{-\beta t})$ was substituted into Eq. 5. The elimination data were then NONLIN fitted to Eq. 5, iterating five parameters: Cl_{CSF}, A, B, α, and β.

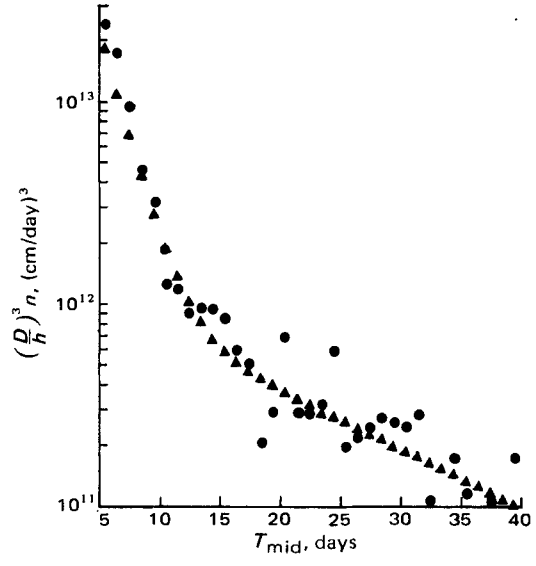

Figure 8—*Predicted (▲) and observed (●) particle number factor [(D/h)³n] versus midpoint times for II*d*. The predicted values were derived from the NONLIN biexponential equation of the particle number factor. The observed values were derived from Eq. 6, which utilizes the daily elimination rate data and the NONLIN-calculated apparent cerebrospinal fluid clearance.*

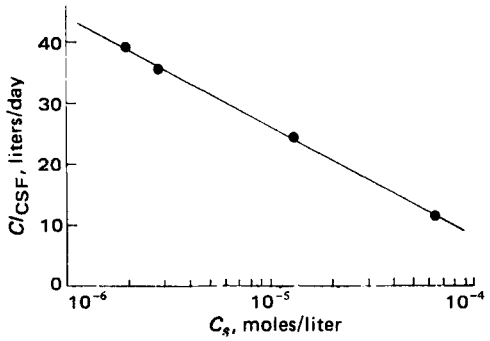

Figure 9—*Plot of the water solubilities of the four compounds versus their apparent cerebrospinal fluid clearance.*

With the NONLIN-derived value for Cl_{CSF}, $[(D/h)^3n]$ can be generated by rearranging Eq. 5:

$$\left[\left(\frac{D}{h}\right)^3 n\right] = \frac{\text{density}^2}{9\pi} \left[\frac{Cl_{CSF}\left(\dfrac{dA_e}{dt}\right)}{\left(C_s Cl_{CSF} - \dfrac{dA_e}{dt}\right)(ARE_{i-1} + ARE_i)^{2/3}}\right] \qquad \text{(Eq. 6)}$$

The plot of $[(D/h)^3n]$ *versus* T_{mid} of II*d* (calculated from Eq. 6) can be compared (Fig. 8) to the NONLIN-parameter-derived values of the biexponential equation. The biexponential equation gives a reasonable empirical approximation for this parameter.

All four compounds were then NONLIN fitted to Eq. 5; data fits can be seen in Figs. 2–5. Parameter values are summarized in Table VIII. The fits are applied to the mean elimination rate data of each of the four compounds.

For comparison purposes, the elimination rate data also were NONLIN computer fitted to a series of model-independent polyexponential equations. A simple model-independent biexponential expression was found to describe accurately the observed data. Table IX illustrates the comparison between the sets of NONLIN fitting with respect to the weighted sum of squares deviations. The dissolution rate-limited model gave equal or only slightly better fits to the data. However, the dissolution rate-limited model has at least one advantage in that it predicts decreasing elimination rates with decreasing water solubilities.

In addition, an interesting correlation exists between the nonrate-limiting Cl_{CSF} parameter and the compound's water solubilities (Fig. 9) and projected octanol–water partition coefficients (Fig. 10). These correlations ($r^2 > 0.999$) predict that the water solubilities of other oils possibly could be large enough for the rate-limiting elimination step to become the passage through the lipid blood–brain barrier rather than dissolution into the cerebrospinal fluid. This behavior is consistent with the Hansch postulates pertaining to drug transport and distribution for biological activity within a series of analog compounds (6–8).

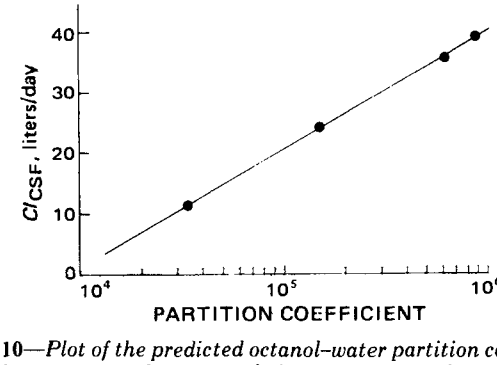

Figure 10—*Plot of the predicted octanol–water partition coefficients of the four compounds versus their apparent cerebrospinal fluid clearance.*

No other correlation was found between water solubilities and other observed or derived parameter values.

CONCLUSIONS

Within the chain length series of C_2–C_6, the decrease of elimination rates and disposition rate constants with increasing chain length was demonstrated. This observation is consistent with a dissolution rate-limited elimination model. Such a model was derived and successfully NONLIN computer fitted to the observed elimination data. The model-derived parameter of clearance from the cerebrospinal fluid through the lipid blood–brain barrier correlated well with the compound's water solubilities and projected octanol–water partition coefficients. Additional compounds need to be tested to evaluate the postulated model system.

REFERENCES

(1) B. W. McKee, R. Ethier, J. L. Vezina, and D. Melacon, *Am. J. Roentgenol.*, **107**, 612 (1969).

(2) B. N. Newton, *J. Med. Chem.*, **19**, 1362 (1976).

(3) A. A. Moss, L. Kaufman, and J. A. Nelson, *Invest. Radiol.*, **7**, 335 (1972).

(4) A. Noyes and J. Whitney, *J. Am. Chem. Soc.*, **19**, 930 (1897).

(5) C. M. Metzler, "NONLIN, A Computer Program for Parameter Estimation in Nonlinear Situations," Upjohn Co., Kalamazoo, Mich., 1969.

(6) C. Hansch and T. Fujita, *J. Am. Chem. Soc.*, **86**, 1616 (1964).

(7) C. Hansch and W. J. Dunn, III, *J. Pharm. Sci.*, **61**, 1 (1972).

(8) C. Hansch and J. M. Clayton, *ibid.*, **62**, 1 (1973).

Distribution and Elimination of Poly(methyl-2-^{14}C-methacrylate) Nanoparticle Radioactivity after Injection in Rats and Mice

JÖRG KREUTER *x, ULRICH TÄUBER ‡, and VOLKER ILLI ‡

Received December 22, 1978, from the **School of Pharmacy, Swiss Federal Institute of Technology, CH-8092 Zürich, Clausiusstr. 25, Switzerland,* and the ‡*Research Laboratories of Schering AG, Berlin/Bergkamen, Germany.* Accepted for publication June 5, 1979.

Abstract □ The organ distribution of poly(methyl-2-^{14}C-methacrylate) nanoparticles after 0.5, 1, 2, 6, and 24 hr and after 7 days, as well as the elimination of degradation products in urine, feces, and breath, was measured for 7 days after intravenous administration to rats. The radioactivity was determined quantitatively after preparation of the organs and qualitatively by macroautoradiography. In addition, nanoparticle distribution after intramuscular administration to mice was determined by macroautoradiography after 7, 35, and 70 days. Thirty minutes after intravenous administration, the nanoparticles were found in the lungs in high concentrations (758 μg/g fresh weight ≅ 22% of the administered dose); 60% (261 μg/g) of the dose was found in the liver. During the first 7 days, the concentration in the lungs decreased from 758 to 284 μg/g while the concentration in the liver increased from 261 to 372 μg/g (≅ 68% of the administered dose), the concentration in the spleen increased from 33 to 131 μg/g (≅ 4%), and the concentration in the bones increased from 3 to 6 μg/g. In all other organs and tissues, the radioactivity decreased significantly. During the first 7 days after intravenous administration, 1% of the administered dose was eliminated in the urine, 3.5% in the feces, and 1% in the breath. After intramuscular administration, all of the ^{14}C-radioactivity still present in the body persisted at the injection site for 70 days.

Keyphrases □ Poly(methyl methacrylate) nanoparticles—distribution and elimination, intravenous and intramuscular administration, radioactive tracer study, rats, mice □ Nanoparticles—poly(methyl methacrylate), elimination and distribution, intravenous and intramuscular administration, rats, mice □ Methyl methacrylate—polymers, distribution and elimination, intravenous and intramuscular administration, rats, mice

During the past few years, nanoparticles and nanocapsules were introduced as new drug delivery systems (1–4). Poly(methyl methacrylate) nanoparticles with incorporated or adsorbed antigens seem to be especially promising as adjuvants for immunology (1, 2, 5, 6). Incorporation into, as well as adsorption onto, these particles yielded much higher antibody titers than aluminum hydroxide and fluid vaccines and gave better protection (1, 5, 6).

Poly(methyl methacrylate) has been used in surgery for over 30 years as a material for artificial bones (7). Implanted poly(methyl methacrylate) seemed to be well tolerated if the implants were monomer-free and under a certain threshold size (8–11).

However, little is known about the biodegradability and the elimination of poly(methyl methacrylate) from the body. Oppenheimer *et al.* (12) implanted small pieces of poly(^{14}C-methyl methacrylate) films [—$CH_2C(CH_3)$-$COO^{14}CH_3$], having 3.6×10^4 cpm/mg, into rats. The rats began to excrete radioactive material after 54 weeks. When the film was removed, the urinary radioactivity disappeared. These investigators concluded that the radioactivity could not be due to any residual monomer in the films since no radioactive material appeared in the urine immediately upon embedding but only after an extended interval. Tomatis (13) implanted poly(methyl methacrylate) films, with a diameter of 15 mm^2, subcutaneously in mice. The urinary excretion of the label was initially low but slowly increased between 2 and 6 weeks after implantation. It fell suddenly to a minimal amount during the 9th week.

Particles in the nanometer range [nanoparticles and nanocapsules (2, 4)] exhibit a much larger surface area than the implants used by previous investigators. In addition, due to the minute size of the nanoparticles, transport from the site of application might occur even after intramuscular injection or implantation. This study was aimed at gaining information about the fate of these nanoparticles after intravenous and intramuscular administrations.

EXPERIMENTAL

Synthesis of Methyl-2-^{14}C-methacrylate [$CH_2{}^{14}C(CH_3)COOCH_3$] (I)—Compound I was synthesized from 2-^{14}C-acetone[1] by the cyanohydrin procedure (14).

[1] 2-^{14}C-Acetone was prepared by conventional methods starting from barium ^{14}C-carbonate *via* Grignard carboxylation and pyrolysis of lithium 1-^{14}C-acetate (20).

0022-3549/79/1100-1443$01.00/0